On-site calibration of the Raman laser absolute frequency for atom gravimeters

Yao-yao Xu, Jia-feng Cui, Kun Qi, Xiao-bing Deng, Min-kang Zhou, Xiao-chun Duan,* and Zhong-kun Hu†
Ministry of Education Key Laboratory of Fundamental Physical Quantities Measurements, Hubei Key Laboratory of Gravitation and Quantum Physics, School of Physics, Huazhong University of Science and Technology, Wuhan 430074, People's Republic of China

(Received 15 January 2018; published 29 June 2018)

The length standard for atom gravimeters is defined by Raman laser wavelength, which, in turn, depends on the absolute laser frequency. Here we present a method to measure Raman laser frequency based on an atom gravimeter itself, which has an advantage of calibrating the length standard on-site. The calibration utilizes the D_2 line of ^{87}Rb atoms as a reference and takes advantage of the cold atom free fall as well as developed techniques of evaluating hyperfine-level shift within atom gravimeters. A calibration accuracy of 1 part in 10^{10} is achieved for the Raman laser frequency, which constrains the corresponding error below 1 μGal in our gravity measurement.

DOI: 10.1103/PhysRevA.97.063626

I. INTRODUCTION

Absolute gravimeters based on atom interferometry have developed rapidly in recent decades [1–10], becoming competitive with classical falling-corner-cube ones [1,11]. For atom gravimeters, a short-term sensitivity up to 4.2 $\mu\text{Gal}/\sqrt{\text{Hz}}$ (1 $\mu\text{Gal} = 1 \times 10^{-8}$ m/s^2) has been achieved [12], and the capability of consecutive operation for months as well as long-term stability has been demonstrated [3,13]. For future development, studies on integrating atom gravimeters with moving platforms for field surveys or space missions are underway [4,14–20].

In order to measure absolute gravity, various systematic errors have been evaluated [1,21–27], and the present accuracy for atom gravimeters is 3 to 5 μGals. Among these systematic errors, the absolute frequency of the Raman laser used to coherently manipulate the atoms must be scrutinized, because it directly defines the ruler in measuring the atom falling distance. An error of 0.38 MHz for the Raman laser frequency will lead to an error of 1 μGal for gravity measurements using ^{87}Rb atoms. In practice, lasers in atom gravimeters are usually locked to transition lines of atoms confined in vapor cells. However, in the lock section the laser frequency may deviate from the appointed transition line due to external disturbances of the atom energy levels as well as unavoidable experimental imperfections. For example, for a laser lock based on modulation transfer spectroscopy [28,29], a shift of 0.8 MHz induced by residual amplitude modulation has been reported [30]. Hence, it is necessary to calibrate the Raman laser absolute frequency independently, rather than assuming a null frequency shift in the lock section.

The laser absolute frequency can be calibrated by a wavelength meter or an optical comb [31]. However, state-of-the-art commercial wavelength meters, with a precision of about 500 kHz [32], do not meet the requirement of gravimeters with μGal accuracy. Optical combs are expensive and fragile laboratory devices, and it is unpractical to depend on optical combs for moving-platform gravimeters. In Ref. [33] spectroscopy by interaction between lasers and laser-cooled atoms is utilized to measure Rb atom transition lines, where the laser frequency is calibrated by an optical comb. In this work, the transition line of laser-cooled ^{87}Rb atoms is used as a reference, and laser spectroscopy is performed to calibrate the laser absolute frequency. For the calibration, the laser is pulsed on as a depletion light to depopulate free-fall cold atoms from the prepared state. And the frequency dependence of the corresponding depletion is measured, which through spectroscopy thus provides an optical frequency discriminator. Compared to vapor cell atoms used in the laser lock section, for state-prepared free-fall cold atoms used in the calibration, external disturbances are reduced, such as background Doppler broadening and magnetic field effects. Furthermore, laser modulation is typically used to create error signals for laser lock. For frequency measurements performed on the laser-cooled atoms, laser modulation can be absent, and thus any accompanying influence due to modulation is avoided. Moreover, within atom gravimeters, it is convenient to evaluate systematic errors in the calibration, such as Doppler shift, ac-Stark shift, and Zeeman effect. Here we demonstrate a calibration accuracy of 43 kHz for our Raman laser, which corresponds to an uncertainty approaching to 0.1 μGal in gravity measurements.

II. EXPERIMENTAL SETUP

The calibration of laser absolute frequency is carried out in a transportable atom gravimeter and takes advantage of available atomic fountain, state preparation, normalization detection, and so on within the gravimeter. As shown in Fig. 1(a), at the beginning ^{87}Rb atoms are loaded and launched to a height of 0.6 m by a magneto-optical trap. The atomic fountain contains about 10^8 atoms with a temperature of about 7 μK. After the atoms enter the interference chamber, a Raman π pulse is applied to select atoms in the $m_F = 0$ magnetic sublevel as well as to perform the velocity selection. Meanwhile, the Raman π pulse also transfers the selected atoms to the ground state $F = 1$ from the initial $F = 2$ state. Then the remnant atoms in $F = 2$ state are blown away. When the state-prepared atoms are flying

*duanxiaochun2011@hust.edu.cn
†zkhu@hust.edu.cn

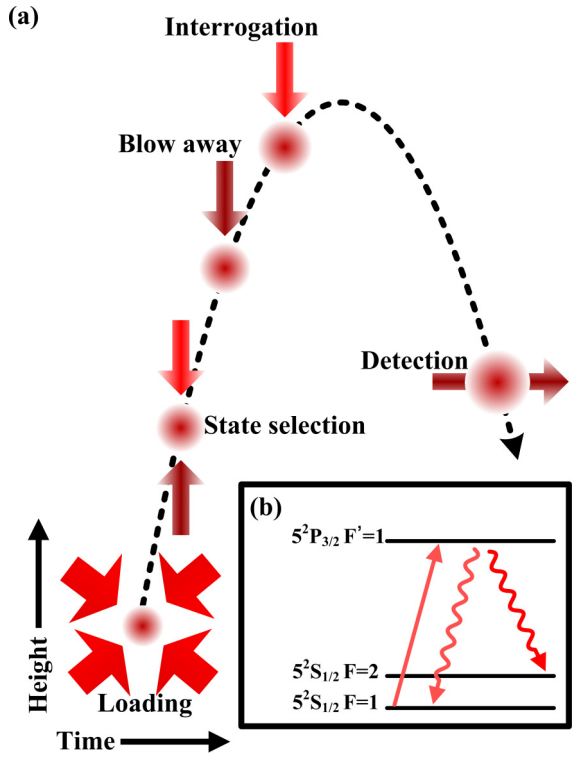

FIG. 1. (a) Schematic of the calibration, which is performed in an atomic fountain. All the manipulating laser beams are available in typical atom gravimeters except for the interrogation laser. (b) The depletion process. After excitation into the excited level $|5^2P_{3/2}, F' = 1\rangle$ by the interrogation laser, the atom will decay into either $|5^2S_{1/2}, F = 2\rangle$ or $|5^2S_{1/2}, F = 1\rangle$.

close to the atomic fountain apex, the laser to be calibrated is pulsed on to interrogate the atoms. This interrogation laser acts as a depletion beam to depopulate the atoms from the $F = 1$ state, as shown in Fig. 1(b). Finally, when the atoms fall back to the detection zone, the population of atoms in the $F = 2$ state is measured by normalized detection, which characterizes the depletion efficiency of the interrogation laser. It takes 1 s to complete the entire process above. From shot to shot, the frequency of the interrogation laser is scanned. And the spectroscopy is obtained by measuring the frequency dependence of the depletion efficiency, which realizes an optical frequency discriminator for the interrogation laser. It is worth noting that the whole calibration process described above can be conveniently implemented within a typical atom gravimeter.

The Raman laser is generated by two external cavity diode lasers for our gravimeter, as shown in Fig. 2. The master laser (ML) is locked to the D_2 transition line of ^{87}Rb atoms by MTS. The ML frequency is supposed to match the transition line between the $F = 2$ and $F' = 3$ states, which, however, requires rigorous evaluation as discussed in the introduction. Before lock, an acoustic-optical modulator (AOM2) shifts the laser frequency up by 264.0 MHz in a double-pass configuration. The AOM2 can be also employed to alter the ML frequency by several MHz. The slave laser (SL) is locked to the ML through an optical phase-locked loop (OPLL), and a microwave source as well as a signal generator is used to provide the effective reference frequency f_{OPLL} for the OPLL. Thus, the SL frequency f_S is related to the ML frequency f_M as $f_s = f_M + f_{\mathrm{OPLL}}$, where f_{OPLL} is approximately 6.834 GHz, corresponding to the energy splitting of the two hyperfine ground states $F = 2$ and $F = 1$ [34].

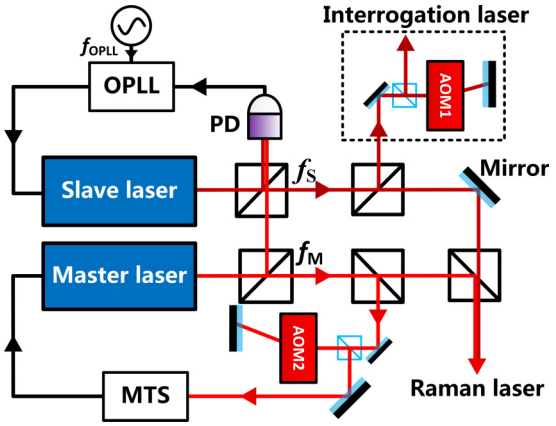

FIG. 2. Schematic of the optical setup. Compared with a typical optical system for atom gravimeters, the only addition is the part as shown in the frame with the dotted line. The subsequent frequency-shift AOMs and the power amplifier for the Raman laser are not shown here. (AOM, acoustic-optical-modulator; MTS, modulation transfer spectroscopy; PD, photodiode; OPLL, optical phase-locked loop).

The output of the two lasers is combined and then amplified by a tapered amplifier. The amplified beam is downshifted by 1500.0 MHz using an AOM to generate the required large detuning for two-photon stimulated Raman transitions. Before coupled into fiber, the Raman laser is further downshifted by an additional 110.0 MHz using another AOM, which acts as a fast switch for the Raman pulses. The two AOMs contribute a total shift of $f_{\mathrm{shift}} = 1610.0$ MHz, and the effective wave vector k_{eff} of the Raman laser is

$$k_{\mathrm{eff}} = 2\pi \times \left(2f_M + f^0_{\mathrm{OPLL}} - 2f_{\mathrm{shift}}\right)/c, \qquad (1)$$

where f^0_{OPLL} is the actual OPLL effective reference frequency in practical gravity measurements, and c is the light speed in vacuum. Since the frequencies of the signal sources driving the OPLL and AOMs can be easily measured to the kHz level, the accuracy of k_{eff} is mainly attributed to the measurement uncertainty of f_M or f_S.

In principle, k_{eff} can be determined by measuring either f_M or f_S, since the two frequencies are connected through the OPLL. Here the SL is chosen as the interrogation laser, since f_S can be easily scanned through the OPLL without changing the interrogation laser beam intensity, even for a large scanning range. As shown in the dotted frame of Fig. 2, the interrogation laser is picked up from the output of the SL, which is guided into the vacuum through the same fiber transmitting the Raman laser. Before being coupled into the fiber, the interrogation laser is downshifted by $f^{\mathrm{AOM1}}_{\mathrm{shift}} = 160.0$ MHz with AOM1, bringing the laser frequency near the resonance on the D_2 transition of the $F = 1$ to $F' = 1$ state. The AOM1 is also used as a fast switch as well as an intensity controller for the interrogation laser. Compared to a normal experimental setup of atom gravimeters, only the interrogation laser is added for the calibration.

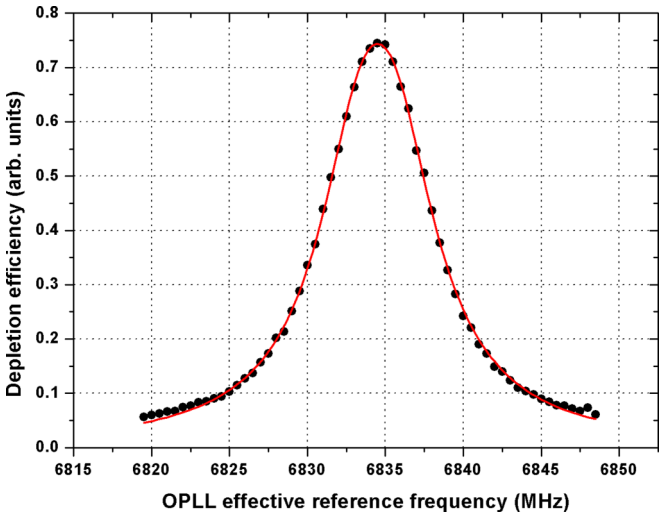

FIG. 3. Typical spectroscopy for the calibration. The horizontal axis shows the OPLL effective reference frequency, which corresponds to the frequency scan of the interrogation laser. The solid line is a fit to the data by the function defined by Eq. (2). The pulse duration as well as the intensity of the interrogation laser is fixed during the frequency scan.

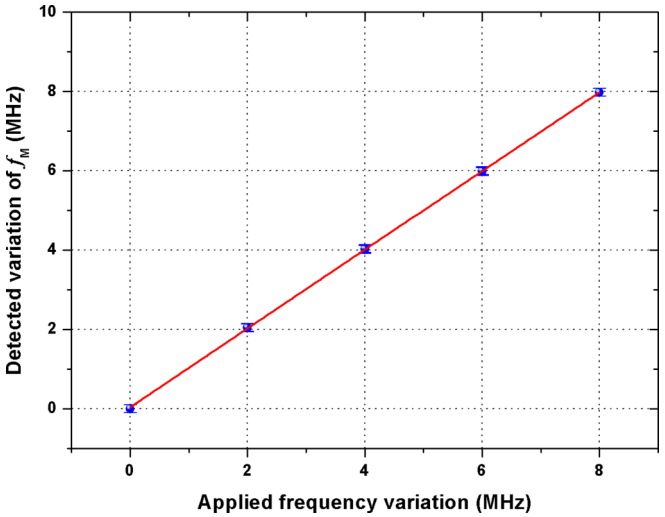

FIG. 4. Variation of the laser frequency detected by the calibration versus a known change of the ML frequency, which is induced by altering the driving frequency of AOM2. The solid line is a linear fit to the data.

III. MEASUREMENTS AND ANALYSIS

The pulse duration and the beam intensity of the interrogation laser are experimentally adjusted to ensure a high contrast for the spectroscopy through the help of AOM1. The optimal pulse duration and beam intensity are found to be approximately 15 μs and 130 μW/cm^2, respectively. The frequency of the interrogation laser is scanned by a step of 0.5 MHz from shot to shot to scan the spectroscopy with the help of the OPLL. Typical spectroscopy is shown in Fig. 3, which exhibits a single-peak spectrum as expected. The center frequency f^r_{OPLL} corresponds to the situation when the interrogation laser is resonant on the transition line. f^r_{OPLL} can be obtained by fitting the spectroscopy with the function

$$1-\exp\left\{\frac{A}{1+\left[4\left(f_{\mathrm{OPLL}}-f^r_{\mathrm{OPLL}}\right)^2/\Gamma^2\right]}\right\}, \qquad (2)$$

where f^r_{OPLL}, line width (Γ), and amplitudes (A) are free parameters [33]. f_M is thus determined as

$$f_M = f_0 + f^{\mathrm{AOM1}}_{\mathrm{shift}} - f^r_{\mathrm{OPLL}} + f^{\mathrm{sys}}_{\mathrm{shift}}, \qquad (3)$$

where f_0 is the optical frequency of $|5^2S_{1/2}, F=1\rangle$ to $|5^2P_{3/2}, F'=1\rangle$ transition for ^{87}Rb atoms, which has been well measured [34]. $f^{\mathrm{sys}}_{\mathrm{shift}}$ accounts for other influences that shift the resonance frequency.

In order to validate the calibration, f_M is intentionally altered by a known amount by changing the driving frequency of AOM2. Meanwhile, the calibration is performed to detect the variation of f_M. The result is shown in Fig. 4, which manifests a linear relation as expected. According to the result of a linear fit, the slope 0.99(1) agrees well with the expected value of 1.

As for determining the absolute optical frequency, $f^{\mathrm{sys}}_{\mathrm{shift}}$ must be evaluated. Compared to atoms confined in vapor cells, there is no large line-width broadening owing to the Doppler effect for cold atoms in a fountain. The inhomogeneous Doppler shift is only about 23 kHz for the atoms prepared by velocity-sensitive Raman selection. However, there is a unitary velocity for atoms in a fountain, which may induce a shift. The unitary velocity can be precisely measured by the velocity-sensitive Raman spectroscopy [35], which gives a result of $v = 0.078(1)$ m/s at the interrogation moment. During the interrogation, a mechanical switch placed above the bottom mirror is temporarily enabled to avoid reflection of the interrogation laser. Thus, the atoms interact only with the down-propagating beam. The corresponding Doppler shift is thus $\vec{k}\cdot\vec{v} = -2\pi \times 100(1)$ kHz, where $\vec{k}$ is the wave vector of the interrogation laser. This wave vector depends on the frequency of the interrogation laser. However, it needs to be known only to a precision of the THz level to calculate the Doppler shift to kHz-level precision. We have also changed the interrogation moment to modulate the Doppler shift, and the corresponding variation of f^r_{OPLL} is measured, as shown in Fig. 5. The induced local gravity acceleration from the slope of linear fit (the slope equals $\vec{k}\cdot\vec{g}$ in theory) is 9.77(8) m/s^2, which agrees well with the measured value by our atom gravimeter.

As shown in Fig. 1(b), the atom is displayed with a three-level structure. In actual atoms, the magnetic sublevels of the three involved hyperfine states should be accounted for, which implies the possibility of a Zeeman shift. In Fig. 3 the result corresponds to a magnetic field of 111 mG with an injection current of 10 mA for the bias coils. This magnetic field will result in a frequency shift of about 111 kHz, if atoms are in the magnetically sensitive sublevel. In order to evaluate the Zeeman shift, the magnetic field is modulated between 110 and 220 mG by a step of 22 mG, while the calibration is carried out synchronously. The measured f^r_{OPLL} shows a peak-to-peak variation up to 26 kHz but without a very regular shift. We suppose it is due to symmetrical structure of the magnetic sublevels.

Off-resonant coupling of the interrogation laser to other D_2 line hyperfine components causes shifts of both

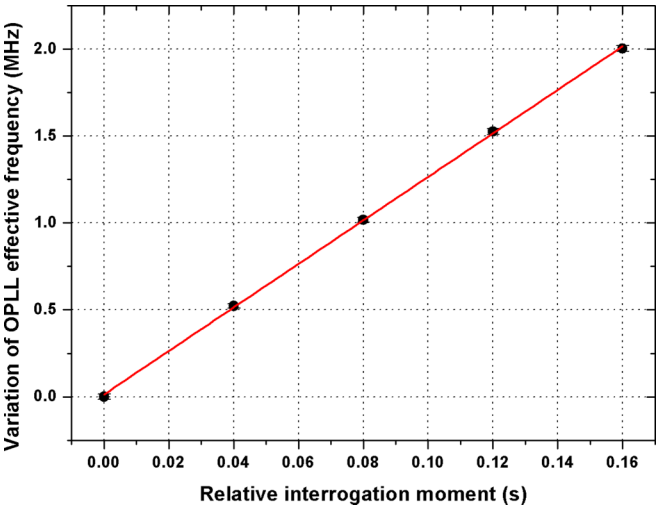

FIG. 5. Variation of the OPLL frequency on resonance when the timing of the interrogation moment is changed, which demonstrates the influence of the Doppler shift. The solid line is a linear fit to the data.

$|5^2S_{1/2}, F = 1\rangle$ and $|5^2P_{3/2}, F' = 1\rangle$, namely, the ac-Stark shift. The ac-Stark shift is theoretically calculated, and the maximum amount is 10.8 Hz/(μW/cm^2). Considering a typical intensity of 130 μW/cm^2 for the interrogation laser in this experiment, the corresponding ac-Stark shift is 1.4 kHz. We attribute this shift as an uncertainty instead of a correction. In addition to the ac-Stark shift, the interrogation laser induces photon recoil, which causes two systematic errors as discussed in Ref. [33]. One is from the recoil energy $E_r = 2\pi\hbar \times$ 3.8 kHz, which shifts the resonance frequency during the interrogation. The other influence is owing to the accelerating effect induced by the absorption-emission cycle, which causes the velocities of the atoms to redistribute. The atoms are initially prepared in $|5^2S_{1/2}, F = 1\rangle$ state, and about 75% of the atoms are repumped to the $|5^2S_{1/2}, F = 2\rangle$ state during the interrogation. Thus, every atom on average absorbs 4.5 photons before being pumped into the nonresonant ground state. The resultant effective shift is approximately 34 kHz, which is also considered as an uncertainty. The systematic shifts above are summarized in Table I, and the total uncertainty is 43 kHz.

With $f_{\text{shift}}^{\text{sys}}$ evaluated, the absolute frequency f_M can be determined. During the 10th International Comparison of Absolute Gravimeters held by National Institute of Metrology (NIM) in Beijing, China, we transported our gravimeter there

TABLE I. Systematic errors in calibrating the laser absolute frequency. All units are in kHz.

Source	Correction	Uncertainty
Doppler shift	−100	1
ac-Stark shift		1.4
Zeeman shift		26
Recoil shift	3.8	
Velocity redistribution		34
Sum	−96.2	43

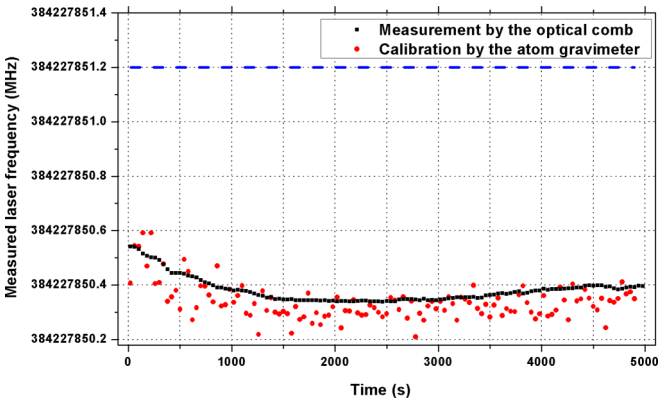

FIG. 6. Laser frequency measured by an optical comb (black squares) and the calibration using an atom gravimeter (red circles). The origin of the horizontal axis is the locking time. The two results agree well with each other but are far from the supposed value (blue dash line) with null shift assumed in the lock section.

to attend the comparison, and a NIM optical comb is utilized to examine the accuracy of the calibration. Figure 6 shows the consecutive calibration result of f_M using our gravimeter along with the result measured simultaneously by the optical comb, where one measurement point takes 40 s. If the laser is exactly resonant on the transition line of $F = 2$ to $F' = 3$ based on the MTS in the lock section, f_M is supposed to be 384 227 851.2 MHz [34] (displayed in Fig. 6 as a dashed line). The data from our gravimeter are shown by red circles, and the data by the optical comb are shown by black squares. It is clearly shown that the result by the calibration using the atom gravimeter is in reasonable agreement with that by the optical comb. The average value of the difference between the two results is (-40 ± 43) kHz. With f_M determined, the effective wave vector k_{eff} can be calculated based on Eq. (1). According to $\Delta g/g = \Delta k_{\text{eff}}/k_{\text{eff}}$, an accuracy of 43 kHz for f_M corresponds to an uncertainty of 0.1 μGal for gravity measurements, which is quite acceptable for present atom gravimeters. According to the difference between the measured value and the assumed value as shown in Fig. 6, the error of f_M may reach 0.8 MHz without calibration, which would lead to an uncertainty of 2 μGal. We also performed a measurement of f_M with an optical comb in our own laboratory earlier [36], and the measured value deviated by about 0.6 MHz from the appointed line. Thus there is not only possible deviation between actual and assumed frequencies for Raman laser, but also possible variation of the deviation in different environments, which confirms the necessity of on-site calibration.

IV. DISCUSSION AND CONCLUSIONS

In Fig. 6 there is an obvious fluctuation of the laser frequency, especially at the beginning of the lock. It is suspected that the laser beam power in the generation of the MTS would affect the laser lock, which is investigated by a modulation experiment. In the modulation experiment, the power of the drive signal for AOM2 is varied to modulate the diffraction efficiency, which, in turn, changes the beam power used to generate the MTS. The corresponding variation of f_M versus the beam power is detected by the calibration, while the drive

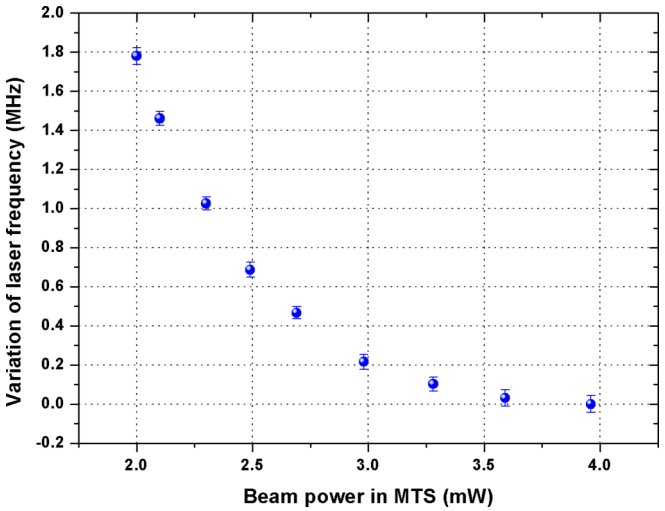

FIG. 7. Variation of f_M versus the modulation of the beam power used to generate the MTS.

frequency for AOM2 is fixed. The result is shown in Fig. 7, which indicates an obvious dependence of f_M on the beam power, especially for insufficient beam power. The variation on f_M even reaches 2 MHz.

In conclusion, we demonstrate an on-site calibration of Raman laser absolute frequency for atom gravimeters, which is capable to constrain the corresponding error below 1 μGal. The calibration takes the transition line of free-fall cold atoms as a clean optical frequency discriminator. State preparation as well as normalization detection helps further improve the spectroscopy. Moreover, in an atomic fountain, it is convenient to evaluate the Doppler shift, Zeeman shift, and ac-Stark shift for the calibration. What's more important is that the calibration can be carried out within an atom gravimeter by only adding an interrogation laser beam. We believe this work is illuminating for the development of inertial sensors by atom interferometry, especially for moving-platform-based ones.

ACKNOWLEDGMENTS

The authors would like to thank Zehuang Lu and Jie Zhang for discussions regarding optical frequency measurement, and Shun Wang for revising the English in this version. We would also like to thank Shuqing Wu, Wei Zhuang, Yang Zhao, and Shaokai Wang of the National Institute of Metrology, China, for their help with optical comb measurement. This work is supported by the National Natural Science Foundation of China (Grants No. 11727809, No. 11625417, and No. 11574099).

[1] A. Peters, K. Y. Chung, and S. Chu, Metrologia **38**, 25 (2001).
[2] J. Le Gouët, T. E. Mehlstäubler, J. Kim, S. Merlet, A. Clairon, A. Landragin, and F. P. Dos Santos, Appl. Phys. B **92**, 133 (2008).
[3] H. Müller, S. W. Chiow, S. Herrmann, S. Chu, and K. Y. Chung, Phys. Rev. Lett. **100**, 031101 (2008).
[4] Q. Bodart, S. Merlet, N. Malossi, F. P. Dos Santos, P. Bouyer, and A. Landragin, Appl. Phys. Lett. **96**, 134101 (2010).
[5] R. Charrière, M. Cadoret, N. Zahzam, Y. Bidel, and A. Bresson, Phys. Rev. A **85**, 013639 (2012).
[6] M. Andia, R. Jannin, F. Nez, F. Biraben, S. Guellati-Khélifa, and P. Cladé, Phys. Rev. A **88**, 031605 (2013).
[7] M. K. Zhou, Z. K. Hu, X. C. Duan, B. L. Sun, L. L. Chen, Q. Z. Zhang, and J. Luo, Phys. Rev. A **86**, 043630 (2012).
[8] S. Abend, M. Gebbe, M. Gersemann, H. Ahlers, H. Müntinga, E. Giese, N. Gaaloul, C. Schubert, C. Lämmerzahl, W. Ertmer, W. P. Schleich, and E. M. Rasel, Phys. Rev. Lett. **117**, 203003 (2016).
[9] X. Wu, F. Zi, J. Dudley, R. J. Bilotta, P. Canoza, and H. Müller, Optica **4**, 1545 (2017).
[10] G. W. Biedermann, H. J. McGuinness, A. V. Rakholia, Y. Y. Jau, D. R. Wheeler, J. D. Sterk, and G. R. Burns, Phys. Rev. Lett. **118**, 163601 (2017).
[11] S. Merlet, Q. Bodart, N. Malossi, A. Landragin, F. P. Dos Santos, O. Gitlein, and L. Timmen, Metrologia **47**, L9 (2010).
[12] Z. K. Hu, B. L. Sun, X. C. Duan, M. K. Zhou, L. L. Chen, S. Zhan, Q. Z. Zhang, and J. Luo, Phys. Rev. A **88**, 043610 (2013).
[13] A. L. Chauvet, T. Farah, Q. Bodart, A. Clairon *et al.*, New J. Phys. **13**, 065025 (2011).
[14] T. Könemann, W. Brinkmann, E. Göklü *et al.*, Appl. Phys. B **89**, 431 (2007).
[15] M. Schmidt, A. Senger, M. Hauth, C. Freier, V. Schkolnik, and A. Peters, Gyroscopy Navigation **2**, 170 (2011).
[16] Y. Bidel, O. Carraz, R. Charrière, M. Cadoret, N. Zahzam, and A. Bresson, Appl. Phys. Lett. **102**, 144107 (2013).
[17] H. Müntinga, H. Ahlers, M. Krutzik *et al.*, Phys. Rev. Lett. **110**, 093602 (2013).
[18] T. Farah, C. Guerlin, A. Landragin, P. Bouyer, S. Gaffet, F. P. Dos Santos, and S. Merlet, Gyroscopy Navigation **5**, 266 (2014).
[19] B. Wu, Zhaoying Wang, B. Cheng, Q. Y. Wang, A. P. Xu, and Q. Lin, Metrologia **51**, 452 (2014).
[20] B. Barett, L. A. Micollier, L. Chichet, B. Battelier, T. Leveque, A. Landragin, and P. Bouyer, Nat. Commun. **7**, 13786 (2016).
[21] A. Gauguet, T. E. Mehlstaubler, T. Lévèque, J. Le Gouët, W. Chaibi, B. Canuel, A. Clairon, F. P. Dos Santos, and A. Landragin, Phys. Rev. A **78**, 043615 (2008).
[22] S. Y. Lan, P. C. Kuan, B. Estey, P. Haslinger, and H. Muller, Phys. Rev. Lett. **108**, 090402 (2012).
[23] S. Zhan, X. C. Duan, M. K. Zhou, H. B. Yao, W. J. Xu, and Z. K. Hu, Opt. Lett. **40**, 29 (2015).
[24] B. Cheng, P. Gillot, S. Merlet, and F. P. Dos Santos, Phys. Rev. A **92**, 063617 (2015).
[25] M. K. Zhou, Q. Luo, L. L. Chen, X. C. Duan, and Z. K. Hu, Phys. Rev. A **93**, 043610 (2016).
[26] M. K. Zhou, L. L. Chen, Q. Luo, K. Zhang, X. C. Duan, and Z. K. Hu, Phys. Rev. A **93**, 053615 (2016).
[27] Y. J. Tan, C. G. Shao, and Z. K. Hu, Phys. Rev. D **95**, 024002 (2017).
[28] J. H. Shirley, Opt. Lett. **7**, 537 (1982).
[29] D. J. McCarron, S. A. King, and S. L. Cornish, Meas. Sci. Technol. **19**, 105601 (2008).

[30] E. Jaatinen and D. J. Hopper, Optics Lasers Eng. **46**, 69 (2008).
[31] S. T. Cundiff and J. Ye, Rev. Mod. Phys. **75**, 325 (2003).
[32] HighFinesse wavelength meter, http://www.highfinesse.com/en/wavelengthmeter.
[33] M. Maric, J. J. McFerran, and A. N. Luiten, Phys. Rev. A **77**, 032502 (2008).
[34] Daniel A. Steck, Rubidium 87 D Line Data, http://steck.us/alkalidata (revision 2.0.1, 2 May 2008).
[35] K. Moler, D. S. Weiss, M. Kasevich, and S. Chu, Phys. Rev. A **45**, 342 (1992).
[36] J. Zhang, Z. H. Lu, Y. H. Wang, T. Liu, A. Stejskal, Y. N. Zhao, R. Dumke, Q. H. Gong, and L. J. Wang, Laser Phys. **17**, 1025 (2007).